Dynamic Friction Co-efficient of Asymmetrical Friction Connections (AFC)

2013 NZSEE Conference

R. Herve, G.W. Rodgers, J.G. Chase, J. Chanchi, & G.A. MacRae

Departments of Mechanical and Civil Engineering, University of Canterbury, Christchurch.

G.C. Clifton

Department of Civil Engineering, The University of Auckland, New Zealand.

ABSTRACT: Asymmetrical Friction Connections (AFC) have been developed as low to no damage damping solutions. Low damage structures require alternative methods of dissipating response energy to avoid excessive displacement response. The AFC device concept is based on energy dissipation during an earthquake through friction. AFC devices are subject to a range of different forces that can lead to a loss of efficiency. In particular, the bolts of the connection that provide the clamping force to the friction interface can be subject to yielding, reducing the normal force and thus frictional resistive force provided by the AFC. This degradation must be characterised to generate safe designs since many structures undergo significant aftershocks within minutes or hours of a major event. Tests carried at the University of Canterbury recorded the dynamic elongation of these bolts during a range of controlled cyclic loading amplitudes. An LVDT placed across the retaining bolts provided a measurement of the dynamic strain in the bolts during movement of the friction interface.

This paper describes the effect of the initial torque value of the bolts on the axial force and resulting friction coefficient for a generic AFC device. A noticeable effect of this assembly torque level on the axial force of the bolts, which yield/plastically deform for initial torque values above 200Nm, is that the maximum axial force observed during testing increases relatively slowly compared to the increase of initial torque value. The results also show a heretofore unobserved dependence of the friction coefficient and device force on the direction of sliding. Finally, the dynamic friction coefficient derived from this model and analysis was consistent across all initial assembly torques, validating the overall analysis and methods. The overall results serve to better characterise these emerging, novel energy dissipation devices.

1 INTRODUCTION

Beyond the immediate effects of a large earthquake, the recent seismic events in Christchurch have shown the major effects damage and downtime can have on a society. The economic disruption over the long rebuild period has a major influence on a city. Therefore, there is a significant drive to develop low damage structural connections that do not lead to the need for major repair or rebuild after a large earthquake. This manuscript focuses on characterising the dynamic performance of the Asymmetrical Friction Connection (also referred to broadly as the Sliding Hinge Joint (SHJ)) which dissipates energy during an earthquake through a sliding friction interface at the beam-column connection.

This work focuses on analysing results from experimental tests carried out on AFC devices at the University of Canterbury to determine the dynamic clamping effects. The tests focused on the behaviour of the clamping bolts and aimed to characterise the dynamic friction coefficient of the connection.

1.1 **Asymmetrical Friction Connection (AFC) mechanics**

Figure 1 presents the SHJ which is a combination of plates of different materials, which are assembled to dissipate seismic energy. This friction connection has been developed as a low-cost, efficient means to protect structures from earthquakes. The manufacturing process of SHJs is straightforward, and the friction mechanism enables the repeatable dissipation of seismic energy to keep the structure in the elastic domain without damaging the overall connection. The end result is minimal damage, where typical rigid fixed connections may have yielded to dissipate energy, resulting in significant damage and economic loss. Ultimately, the SHJ provides an alternate energy dissipation mechanism to the yielding of steel frame elements and the formation of plastic hinge zones. The SHJ (also called Asymmetrical Friction Connections or AFC) was initially developed by Clifton (2005) and have been tested in many studies since (Golondrino et al (2012a, 2012b), Clifton et al (2004, 2007), Khoo et al (2012)).

a) Disassembled device *b) Assembled device*

Figure 1: Details of the Asymmetrical Friction Connection device.

The SHJ consists of three steel plates and two shims held together with bolts, as shown in Figure 1. The two long plates are called the moving plate and the top plate. They are drilled, enabling them to be fixed on both sides of the beams and columns to which they connect. The slots within the moving plates enable the mechanism to translate when the beam and the column move.

The movement of the moving plate generates friction forces in the interface between the moving plate and the shims, which propagates into the extremity of the mechanism (top and cap plates). Static and kinetic friction forces are dependent on the shim materials used and construction quality. Bolt tension is a particularly sensitive parameter in determining the resulting normal force on the shim and thus the actual connection dissipation force.

2 **METHODS**

2.1 **Experimental Methods**

An AFC device was assembled with a 220mm slot, using Grade 300 steel plates, Bisalloy 500 shims, Belleville washers, and M16 Grade 8.8 galvanized bolts with 110mm length. Different connections assembled using a torque control method were tested with the following bolt torque values: 20, 50, 150, 250, 350, 410 and 500 Nm, which is 6.7 - 166.7 % of the 300 Nm proof torque load for the specified bolts. Testing was carried out on a shaking table using a horizontal setup instrumented with a load cell and potentiometer across the connection and a vertical potentiometer installed on the bolt, as shown in Figure 2. The sliding mechanism was initiated by applying a displacement regime on the slotted plate connected to the shaking table. The input displacement regime was composed of 21 sinusoidal cycles with 3 cycles at 7 different increasing amplitudes varying from 3.13 to 100% (1.42-220 mm) of the connection slot length, with a maximum velocity of 15mm/s, as shown in Figure 3 (Golondrino et al (2012b)).

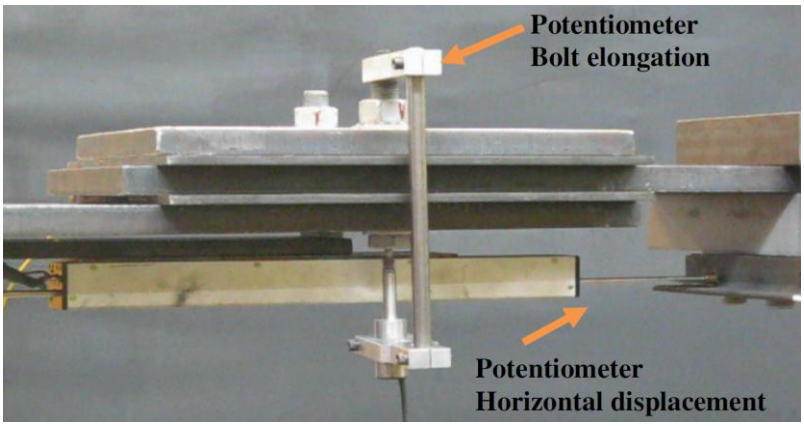

Figure 2: Experimental AFC set-up showing instrumentation localised to the sliding interface.

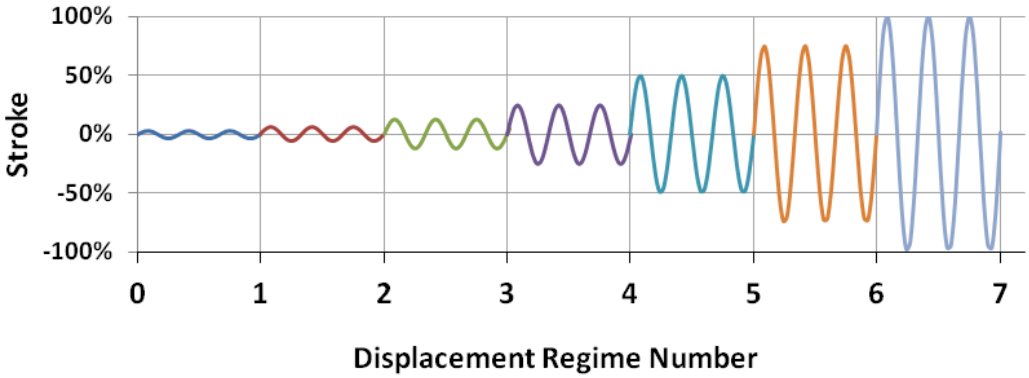

Figure 3: The input displacement loading regime for the experimental specimens.

2.2 **Experimental Results**

2.2.1 *Overall Connection Hysteresis*

Figure 4 presents the hysteresis loop for the overall connection resistive force vs. displacement of the AFC specimens for different initial assembly torque values. The shape of the hysteresis loops varies notably depending on the bolt assembly torque value. Some degradation on successive cycles is observed and this trait is more pronounced for the higher assembly torque values.

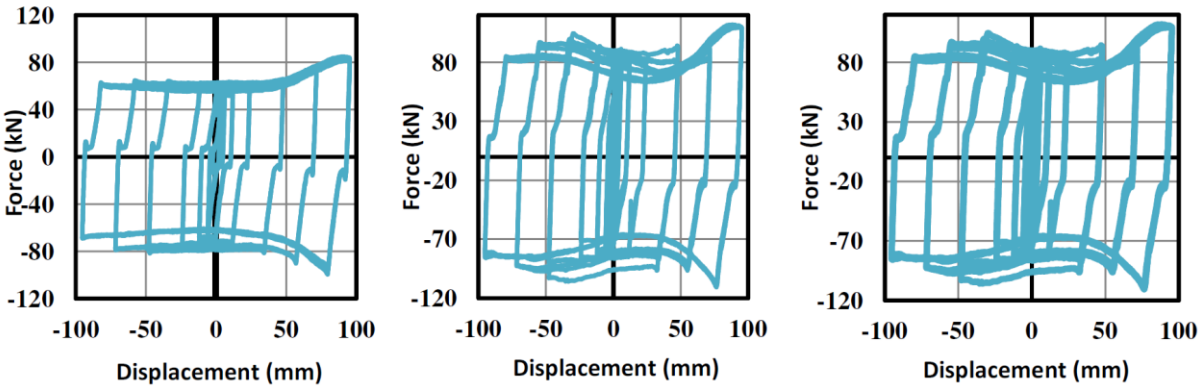

a) Torque 20 Nm *b) Torque 200 Nm* *c) Torque 450 Nm*

Figure 4: Hysteresis loops of AFC connections assembled with different torques values.

The hysteresis loops in Figure 4 show another anomaly compared to the theoretical model near the change of direction. This 'pinching' occurs during initial elastic loading after a change in the direction of the input displacement. The cause of this phenomena is the rotation of the bolt against the plate during the transition between tensile and compression loading. Figure 5 presents two images of the AFC taken during testing which shows the rotation of the bolt which causes the 'pinching' of the hysteresis loop.

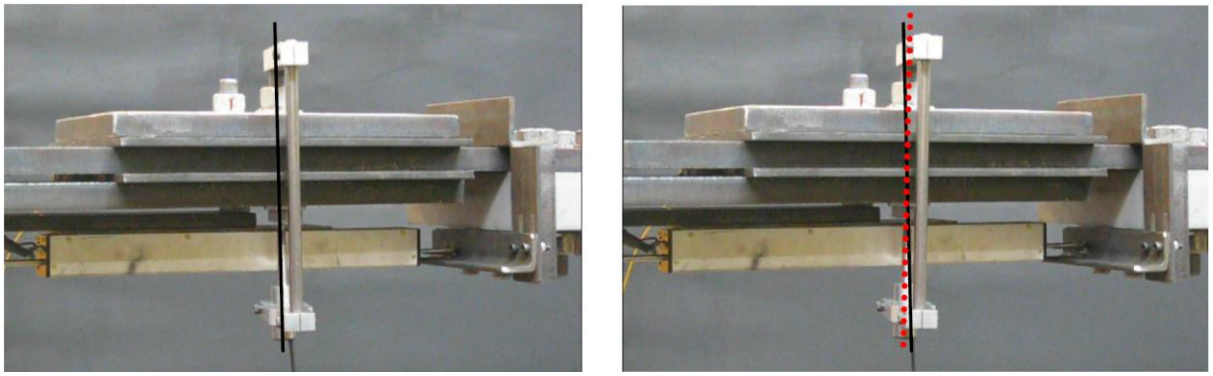

a) Initial position of the bolt

b) Rotated position of the bolt after the transfer from tensile to compressive loading

Figure 5: Bolt rotation during the transition from tensile to compressive loading of the AFC connection.

2.2.2 *Bolt Elongation Measurements*

Figure 6 presents the bolt elongation during cyclic testing of the AFC at a range of different assembly bolt torque values. The data shows two distinct forms. For torque values of 20 to 100 Nm the response shows only some short-duration peak and no offset. However, for assembly torques above 100 Nm, there are notable plateaus in bolt elongation, as well as a gradually increasing drift in bolt elongation.

a) Assembly Torque 20 Nm

b) Assembly Torque 200 Nm

c) Assembly Torque 450 Nm

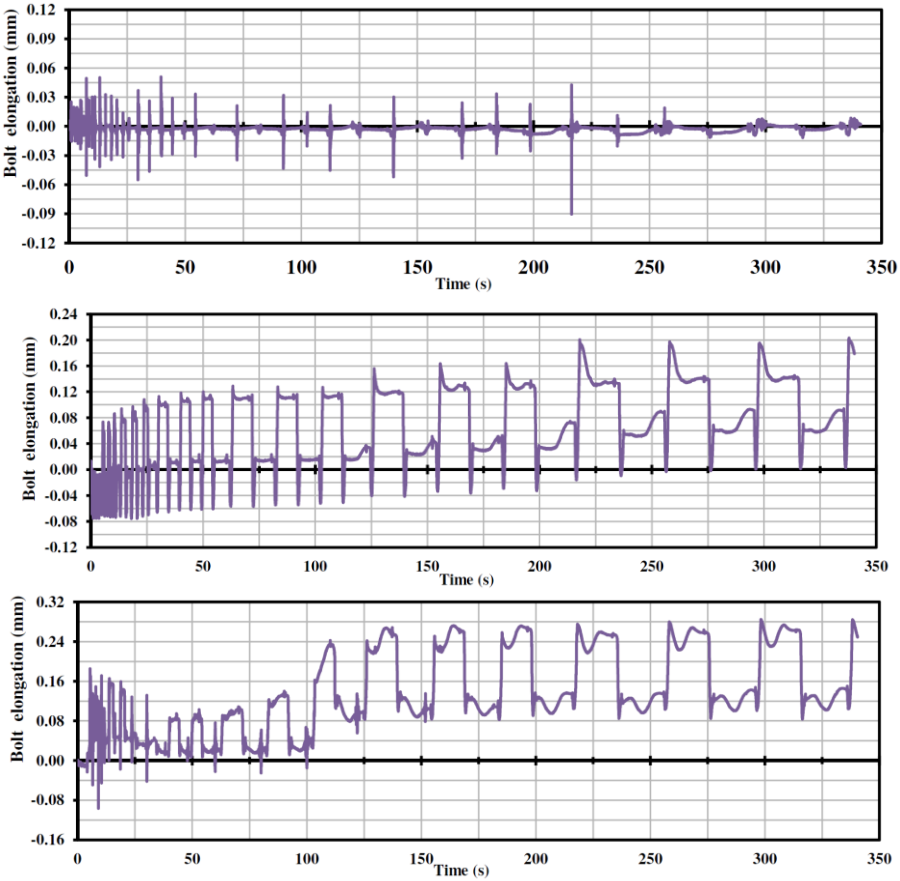

Figure 6: Bolt elongation of AFC connections during cyclic loading for different assembly torque values.

Most notable variations of bolt elongation are located at the change of input direction, as shown in Figure 7 for an assembly torque of 20 Nm. The spikes in bolt elongation seen in Figure 6 are attributed to erroneous readings from bolt rotation rather than bolt elongation, and do not represent true increases in axial strain due to an increase in bolt axial force. In particular, Figure 7 indicates that the large "spikes" seen in Figure 6 do not coincide with the friction "post-yield" region of loading, but occur instead during initial elastic loading after changing of direction. Thus reflecting bolt rotation against the plate.

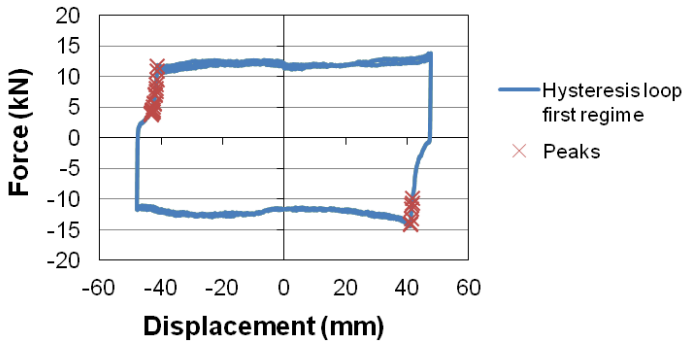

Figure 7: Location of elongation peaks within the hysteresis loop with torque value of 20 Nm, corresponding to the results presented in Figure 6a.

The removed the large localised "spikes" seen in Figure 6, the data is filtered with a low pass filter before it is used to calculate the axial force within to the bolt. The resulting filtered bolt elongation can be used to obtain a dynamic estimate of bolt force during testing and, from that, a dynamic estimate of the friction coefficient at the sliding interface.

2.3 Cycling Loading Model of the Bolt

Axial bolt force recorded during axial tension testing on the bolt can be represented by an elasto-plastic force deflection curve, as shown in Figure 8. The response of the bolt is modelled as a bi-linear response with an initial elastic stiffness K_1 and lower post-yield stiffness, K_2.

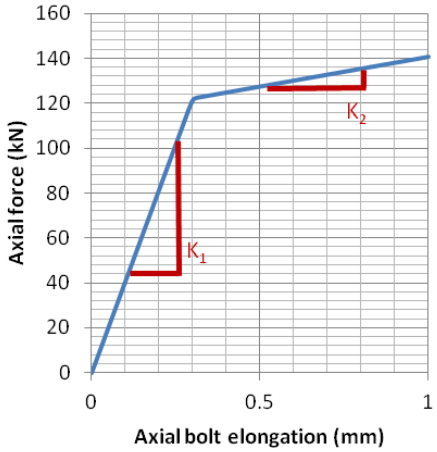

Figure 8: Bolt elongation model fitted to data from axial bolt testing.

A model of the bolt force vs. bolt elongation using the Menegotto-Pinto formulation is defined in Equation 1:

$$F = \frac{K_1(x - x_{reset}) + F_{1,reset}}{\left(1 + \left|\frac{K_1(x - x_{reset}) + F_{1,reset}}{F_{reset}(sign(\dot{x}))}\right|^{\beta}\right)^{1/\beta}} + F_2 \quad (1)$$

$$F_2 = \begin{cases} 0 & if \;\; K_2(x - x_y)sign(\dot{x}) < 0 \\ K_2(x - x_y) & if \;\; K_2(x - x_y)sign(\dot{x}) \geq 0 \end{cases} \quad (2)$$

$$x_y = x_{reset} - \frac{(F_{reset} - F_y \times sign(\dot{x}))}{K_1} \quad (3)$$

where K_1 and K_2 represent elastic and post-yield stiffness coefficients respectively, x is bolt elongation during the test plus the initial elongation induced during assembling process, x_y is the yield displacement, which must be re-calculated each time x_{reset} and F_{1reset} are updated and must be done every time the input velocity changes direction. The value of x_{reset} and F_{1reset} are simply the value of bolt elongation x and force, F_1 when the direction of loading changes sign. The term $sign\ (\dot{x})$ is simply a signum function on the elongation velocity and = 1.0 when $\dot{x}$ is positive and = -1.0 when $\dot{x}$ is negative.

Figure 9 presents the response of the model in Equations (1) – (3). The input motion is the filtered version of the axial elongation measured within the bolt during testing of AFC connection which was presented in Figure 6. Note that bolts yield only occurs for torque values above 200 Nm where the bolt's axial proof load of 95 kN is exceeded during testing.

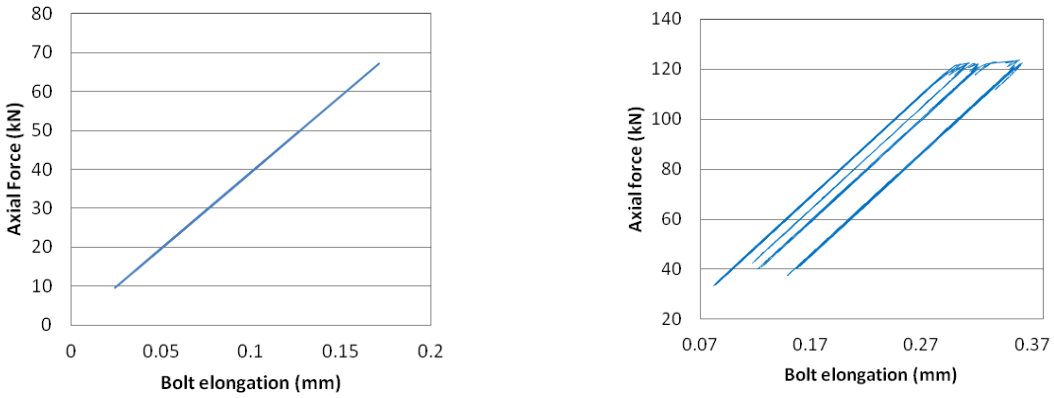

a) Bolt assembly torque – 100 Nm *b) Bolt assembly torque – 200 Nm*

Figure 9: Bolt force calculated from Equations (1) – (3) using measure bolt elongation during testing for different assembly torque values.

2.4 **Determining the Dynamic Coefficient of Friction**

Following a similar approach to MacRae et.al. (2010), the overall connection resistance force, F, can be expressed in terms of the number of shear planes η, the axial force per bolt N, and the friction coefficient between steel and the shim material, μ, as shown Equation 4. For this type of AFC, the number of shear planes is two, yielding:

$$F = \eta \mu N \quad (4)$$

The value of μ can thus be determined for each assembly torque value and experiment.

2.5 **Analyses**

The dynamic coefficient of friction, μ, in Equation (4) is calculated for every experiment. Each experiment was undertaken twice using the input loading profile shown in Figure 3. The bolts were not retightened. Thus, data from the second experiments characterizes degradation.

2.5.1 *Dynamic Co-efficient of Friction Results*

Figure 10 presents the dynamic friction coefficient for an AFC with an assembly torque of 20 Nm for an initial and secondary displacement loading regime. The direction of loading does not have a major influence on the friction coefficient which oscillates around 0.17 for the first run and 0.14 for the second. The periodic drops in friction co-efficient reflect the changes in direction at each input cycle.

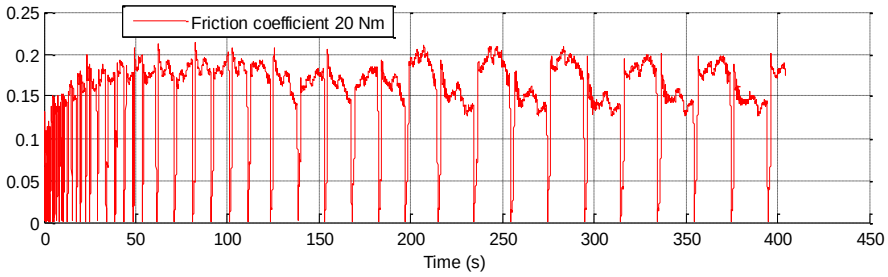

a) First input displacement loading regime (as shown in Figure 3)

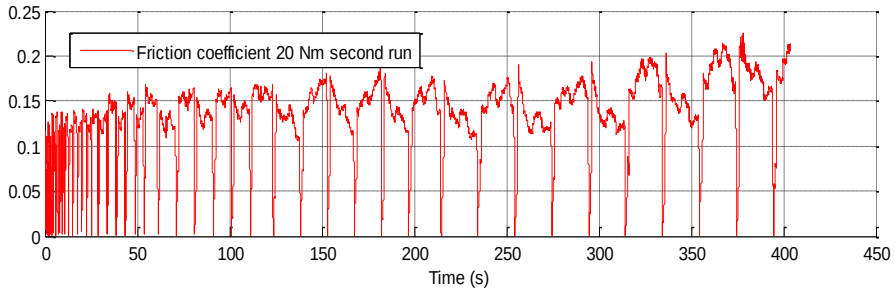

b) Second input displacement loading regime (as shown in Figure 3)

Figure 10: Dynamic friction coefficient during testing (assembly torque = 20 Nm).

Figure 11 presents the dynamic friction coefficient of an AFC with an initial torque of 200 Nm. The value of the friction coefficient during the first run is dependent on the direction of loading with a difference around 0.05 between directions. This behaviour is very regular and μ oscillates around an average of 0.18-0.19. The values of the second run are more consistent and less direction dependant. Degradations can explain the small decrease in the later, larger amplitude cycles.

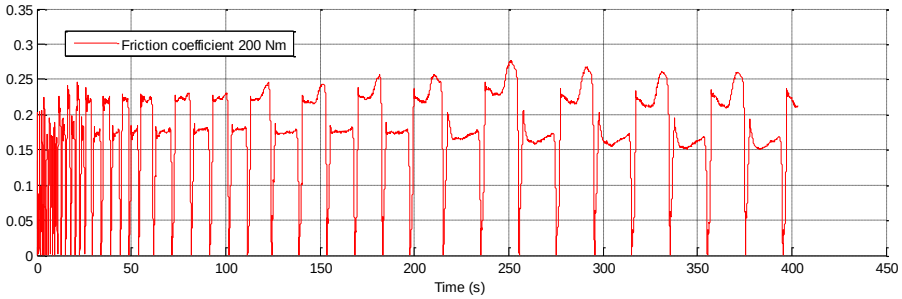

a) First input displacement loading regime (as shown in Figure 3)

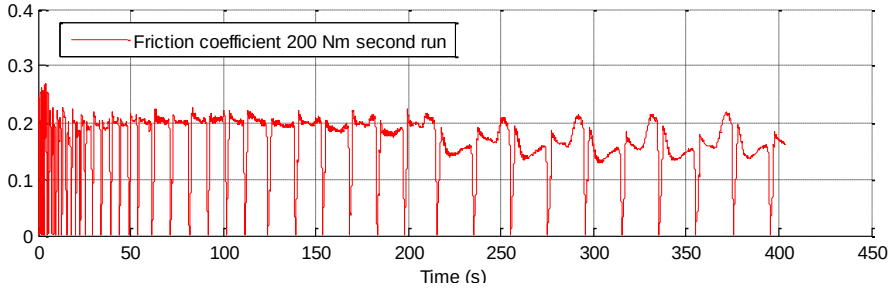

b) Second input displacement loading regime (as shown in Figure 3)

Figure 11: Dynamic friction coefficient during testing (assembly torque = 200 Nm).

2.6 **Overall Analysis**

Overall, the dynamic coefficient of friction varies depending on the initial torque applied to the bolts. Moderate torques of 300-360 Nm produced very stable, consistent values for the dynamic coefficient of friction for the smaller initial displacement cycles. The tests showed much larger variations for the larger amplitude response cycles. Very high and low initial torque values produced much more variable response with a clear directional dependence of the coefficient of friction.

The dynamic friction coefficient is mostly dependent of the direction on sliding, and, as a result, so is the bolt force as shown with the example of 200 Nm torque value in Figure 10. When the shake table pulls the moving part of the device, all plates stay parallel together and the force received by the bolt is "normal". The friction coefficient is now at its higher value. When the shake table pushes the moving part of the device, the plates tend to pull away from each other, reducing the percentage of bolt force that is applied as normal force to the sliding shims. Therefore, the friction coefficient has an apparent lower value. It is difficult to differentiate the percentage of the bolt force that is taken by the separation of the plates and the portion that is applied directly as normal force to the sliding shims.

3 **CONCLUSIONS**

This paper describes the effect of initial bolt assembly torque on the axial force and resulting friction coefficient for a generic AFC device. The bolts are observed to yield for assembly torque values above 200 Nm. The results also show a heretofore unobserved dependence of the friction coefficient and device force on the direction of sliding. Finally, the dynamic friction coefficient derived from this model and analysis was consistent across all initial assembly torques, validating the overall analysis and methods. The overall results serve to better characterise these emerging, novel energy dissipation devices.

4 **REFERENCES**

Golondrino, JC, MacRae, GA Chase, JG, Rodgers, GW, and Mora Munoz, A. (2012a). "Design Considerations for the Braced Frames with Asymetric Friction Connections," STESSA 2012 – Behaviour of Steel Structures in Seismic Areas, Santiago, Chile, January 9-12, 8-pages.

Golondrino, JC, MacRae, GA Chase, JG, Rodgers, GW, and Clifton, G.C. (2012b). "Clamping Force Effects on the Behaviour of Asymmetrical Friction Connections (AFC)" Proceedings of the 15th World Conference on Earthquake Engineering (15WCEE) , Lisbon, Portugal, September 24-28, 8-pages.

MacRae, G.A., Clifton, G.C, Mackinven, H., Mago, N., Butterworth, J., Pampanin, S, (2010) "The sliding hinge joint moment connection" Bulletin of the New Zealand Society for Earthquake Engineering, v 43, n 3, p 202-212.

Clifton, G. C. (2005). "Semi-rigid joints for moment-resisting steel framed seismic-resisting systems," PhD Thesis, The University of Auckland, Auckland, New Zealand.

Clifton GC, MacRae GA, Mackinven H, Pampanin S, Butterworth J.(2007) Sliding Hinge Joints and Subassemblies for Steel Moment Frames, New Zealand Society for Earthquake Engineering Annual Technical Conference, Paper 19, Palmerston North.

Clifton, G. C., Butterworth, J.W., Zaki, R. (2004) "Two New Semi-Rigid Joints for Moment-Resisting Steel Frames", 7th Pacific Structural Steel Conference, Proceedings 7th Pacific Structural Steel Conference, Long Beach, California, March 2004, p.1-14

Khoo H.H., Clifton G.C., Butterworth J., MacRae, G.A. (2012) "Experimental testing of the self-centering sliding hinge joint", Proceedings of the 2012 New Zealand Society for Earthquake Engineering (NZSEE) Annual Technical Conference, Christchurch, New Zealand, 13-15 April 2012